Conference Proceedings

Experimental Momentum-binning for Muon Scattering Tomography

Botond Csatlós,[1 2] Gergő Hamar,[1] Dezső Varga,[1]

[1]*HUN-REN Wigner Research Centre for Physics, Budapest, Hungary*

[2]*Eötvös Loránd University, Faculty of Science, Budapest, Hungary*

Abstract

Muon scattering tomography is a novel cosmic muon imaging technique that exploits the multiple Coulomb scattering of the cosmic muons. Imaging and identification of enclosed high-Z materials become possible and usable in large-volume scanners. The proof of concept is supported via several simulation frameworks and experimental demonstrations. As the scattering angle strongly depends on the momentum of the muon, using that information can enhance the imaging and allow one to expand the identification capabilities toward lower-Z materials. We have constructed a muon-scattering experiment using good spatial resolution 80 cm-size MWPCs, as a multiple-layer setup for precise tracking. The basics of operation have been proved as mapping the scattering strength in 2D/3D maps of targets with various sizes (from 1cm up) and materials (ranging from plastic to lead). The setup is equipped with additional scattering layers below the post target tracking part; scattering on these known layers could indicate the momentum of the incoming muon. This novel method opens for momentum tagging and thus momentum-binned imaging, increasing the discrimination power between materials even in lower-Z region.

Keywords: muon scattering tomography, MST, muography, momentum-binning
DOI: 10.31526/JAIS.2024.496

1. INTRODUCTION

When cosmic radiation encounters the atmosphere of the Earth, it produces hundreds of new particles. When this shower of particles reaches the Earth's surface, it is comprised mainly of muons. Since muons are highly penetrating particles, they allow the imaging of large-sized objects by measuring the reduction of flux due to absorption, which depends on the density and length in a given direction. The first muography experiment was introduced by Alvarez to search for hidden chambers of the Second Pyramid of Giza [1].

In 2003, K. N. Borozdin et al. [2] presented a novel cosmic muon imaging technique called Muon Scattering Tomography (MST) which is based on the multiple Coulomb scattering of the particles. The particle will traverse the material in a stochastic path due to the multiple scatters. The angular scattering distribution is approximately Gaussian, with zero mean. The standard deviation can be described with this formula:

$$\sigma_\theta = \frac{13.6MeV}{p}\sqrt{\frac{x}{x_0}}\left[1 + 0.038\, ln\left(\frac{x}{x_0}\right)\right], \tag{1}$$

where p is the momentum of the incident particle, x is the depth of the material, and x_0 is the radiation length of the material which is strongly sensitive to the atomic number of the target material (x_0 decreases with increasing Z).

This way MST can be used for the separation of low, medium, and large atomic numbers within the samples. Since this is a passive inspection technique, no artificial source of radiation is required, making MST a potential future application in homeland security. Muon Scattering Tomography is an actively researched field today, several simulations and possible applications were demonstrated [3] [4] [5] while a few experiments have been performed for confirmation of the tomography of the internal structure of dense objects.

Performing low-uncertainty measurements is challenging since there can be several orders of magnitude differences in the momentum of the incoming cosmic muons, which is difficult to estimate accurately. However, this is also an advantage because if we can estimate the momentum, we can gather extra information about the targets from the difference in the scattering of particles with different momentum.

2. THE REGARD-MUONSECURITY EXPERIMENT

2.1. Detector construction

The "REGARD-MuonSecurity Experiment" is a 3-meter high, multilayered device consisting of MWPC-based trackers [6] with exceptional operation stability, $>$ 95% tracking efficiency, and good spatial resolution of about 6 mm. The sensitive area is 768 mm x 768 mm for each detector.

A photo and a schematic drawing of the MuonSecurity experiment are shown in Figure 1. An important practical feature is that the position information is measured in two dimensions from signals on individual perpendicular wires. Detector systems consisting of these MWPC-s are currently in use for several scientific and industrial purposes, for example, for volcano muography in the Sakurajima Muography Observatory [7] [8] [9] [10], for underground muography [11] [12], and for geotechnical applications [13] [14] [15].

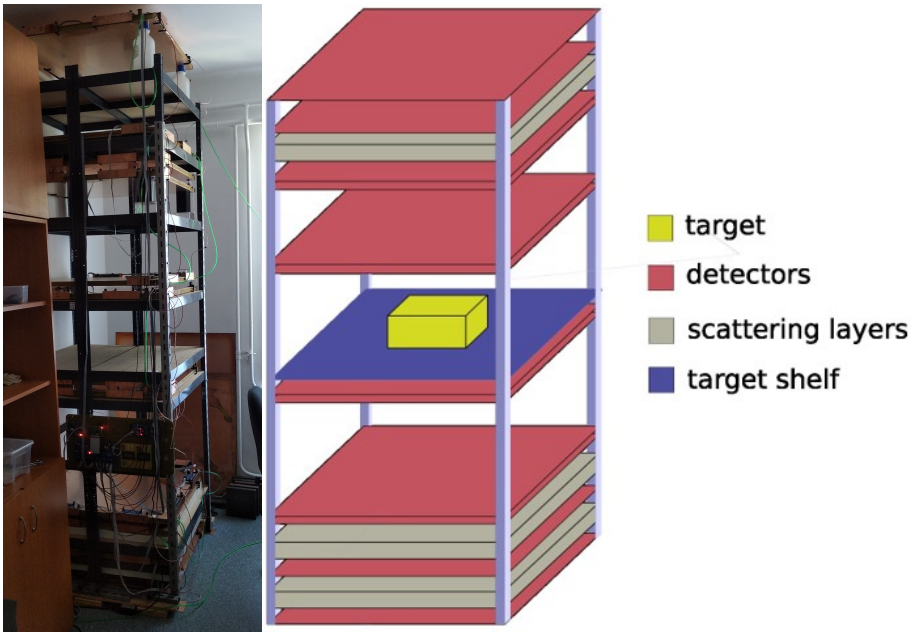

FIGURE 1: A picture and the schematic drawing of the MuonSecurity experiment.

The target plane on which the samples are placed is around the vertical middle. With the used geometrical setup we detect about 30 muon events per second. Considering the position and dimensions of the detectors, the angular resolution is 8 *mRad* while the angle of view is $\approx 30^{\circ}$.

The specialty of the setup is that it contains three scattering layers made of iron. The first layer (2cm) is placed after the entrance of the muon, while the others are placed around the exit part at the bottom with 4 cm and 8 cm thickness. By analyzing the scattering and absorption on these known layers, we can extract information about the momentum of the incoming muon.

2.2. *The imaging process*

The imaging algorithm consists of 4 logically distinct units and works as follows:

(i) *Track reconstruction:* Muons are tracked before and after the target plane using 4+4 layers. The post-target domain is divided into multiple sections allowing us to monitor muons even if they are scattered or absorbed in the scattering layers. From this information, we can infer the momentum of the muons.

(ii) *Eliminating unrelated events:* An event is recorded when at least three of the upper chambers trigger. Therefore, by eliminating all tracks that do not approach another track within a specific distance on the target plane, it becomes easier to identify events when a single muon scatters on a target rather than a shower of particles.

(iii) *Identifying high-angle scatterings:* Higher Z objects tend to produce many high scatterings, so we can enrich the events that happen on the target by eliminating all tracks in which the scattering is less than a specified value. It means that a Heaviside function is being applied to the absolute value of the difference in the slope of the incoming and scattered particle tracks which is bigger than the predefined cut.

(iv) *Imaging:* Partition the target plane into small pads and after counting the number of events that match the previous filter conditions, we normalize each pad's signal by dividing by the original number of rays that passed through that tile.

A quantity shall be defined to simplify cuts and imaging; this "scattering strength" is expressed mathematically using the following formula:

$$\lambda_c = \frac{\sum \Theta(|S^i_{upper} - S^i_{lower}| - c)}{N} \tag{2}$$

where S^i_{upper} and S^i_{lower} are the slope of the track above and under the target shelf in event i, N is the number of hits in the given pad, and c is the angle cut at which the scatterings must be greater than. If we determine the scattering strength over the

FIGURE 2: A picture and the 2D scattering strength map using various samples: lead brick, iron rod, lead glass scintillator, aluminum brick, aluminum rod, wood, and a plastic scintillator.

entire surface of the target plane, the λ map highlights the target. This quantity represents the probability of large-angle scattering occurring over a unit area. In Figure 2, such a distribution is shown, and the c-cut parameter is 30 $mRad$.

The selection of parameter c is arbitrary, yet it plays a huge role in determining the quality of the imaging. If it is too small $(< 20\ mRad)$, then it may not be easy to differentiate the signal from the background, while if it is too large $(> 40\ mRad)$, there might not be enough data to work with, especially in the lower-Z region.

The former images prove that our equipment consisting of the REGARD Group's MWPC-based trackers is capable of producing distinct images for materials of varying atomic numbers, sizes, and compositions. The experiment promises to be worth further development; after a Geant4 simulation, the MuonSecurity will be equipped with dedicated detectors with larger sensitive areas.

3. MOMENTUM-BINNED IMAGING

Achieving momentum-binned imaging is one of the main objectives of the experiment. The momentum of the muons does play a significant role in the scatterings; thus, momentum tagging could provide additional information during the evaluation process. To accomplish this, the MuonSecurity experiment was designed with additional scattering layers below the post-target tracking section. The scattering on these known layers can indicate the momentum of the incoming muon, enabling momentum tagging.

If a muon passes through the detector and is not absorbed by any of the iron layers, it is considered to have "high momentum". On the other hand, if the muon got absorbed in the last layer, it is a "medium-momentum" muon; and if it is absorbed in the layer before, it is a "low-momentum" muon.

The amount of energy deposited by the muon varies across the three layers: in the first layer, it is 33 MeV; in the second layer, it is 66 MeV; in the third layer, it is 137 MeV. An average muon with a momentum of $3-5\ GeV$ should pass smoothly through the entire system. This means that low- and middle-momentum muons are rare; thus, it is most important to determine (and subtract) the background for imaging with those. Figure 3 shows 2 measurements, and Figure 4 shows the images after background subtraction for the medium- and high-momentum muons.

FIGURE 3: In the first measurement, 2 iron (25 mm each) and a lead (150 mm) brick were tested; in the second, iron (65, 30, 15 mm), lead (60, 30, 20 mm), aluminum (55, 30, 15 mm), and copper (15, 10 mm) were tested.

Due to the rareness of low-momentum events, our statistics are moderate; thus, let us now only focus on the middle- and high-momentum imaging capabilities.

The high- and medium-momentum images provide different pieces of information about the targets, and the contrast of the mid-range Z targets gets larger in the middle-momentum image. For the separation of large Z materials, high-momentum events provide significant information, while for medium-momentum events, even simple visual separation shifts to lower atomic numbers, and their relative contrast is enhanced. The difference can be clearly seen in the 9 different target measurements; for the aluminum samples, in the high-momentum image, the average scattering strength of the 1.5 cm thick aluminum sample is $\lambda_H = 0.023$, which is 4.6 % of the maximum value, barely visible in the image, while in the medium-momentum figure, the

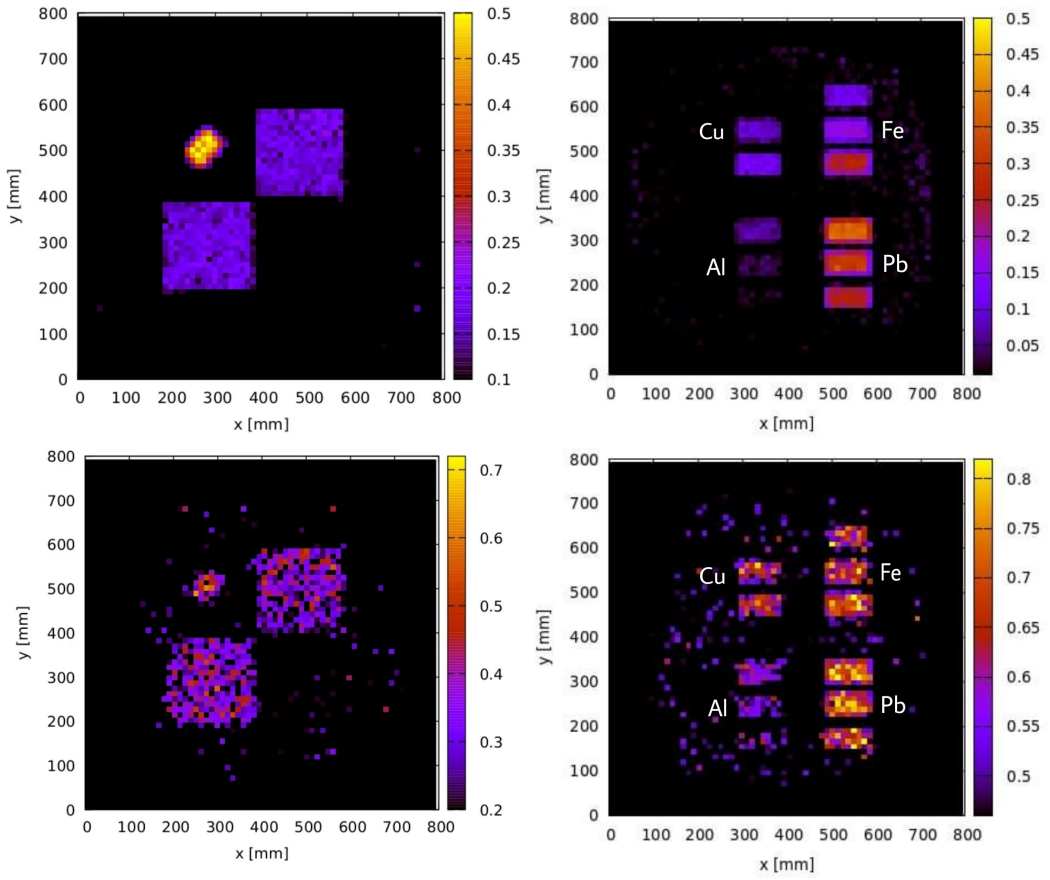

FIGURE 4: The high- and middle-momentum 2D scattering strength map of the above-described measurements.

average scattering strength of the sample is $\lambda_M = 0.051$, 14.7 % of the maximum value, and the sample is more easily identifiable with the naked eye. The same is true for the other two aluminum samples; they are better separated from the background in the medium pulse image. By utilizing the contrast-difference information, imaging can be improved and allow one to expand the identification capabilities toward lower-Z materials.

In order to identify large scatterings and quantify scattering strength more accurately, the Heavyside cut utilized in the definition of scattering strength should be replaced with a more appropriate to the corresponding momentum categories involved.

4. CONCLUSION

The REGARD Group's MuonSecurity experiment is a muon-scattering-tomography setup, constructed from multilayer MWPC tracking layers having good spatial and angular resolution. The setup can be used with a wide range of atomic numbers, in the measurement shown in Figure 2; samples with small (wood), medium (aluminum), and large (lead) atomic numbers were tested simultaneously, giving distinctly different images with good contrast difference.

In this section, we have presented a preliminary study on the momentum-binning, which is an important new element of imaging. New experimental evidence has been presented for a Moun Scattering Tomography system capable of momentum tagging with additional scatter layers; this is unique in the research field and has never been achieved in a muon-scattering experiment before. We have demonstrated the feasibility of momentum-binned imaging which increases the discrimination power between materials even in lower-Z regions making the equipment capable of material classification.

Development of the device is ongoing, and the goal was to carry out preliminary studies for a device that can be used in field applications, for example, in homeland security.

CONFLICTS OF INTEREST

The authors declare that there are no conflicts of interest regarding the publication of this paper.

ACKNOWLEDGMENTS

The authors would like to acknowledge the support of the Hungarian OTKA Grant FK-135349, the ELKH Grant KT-SA-88/2021, and the TKP Grant 2021-NKTA-10. The authors would like to thank the work and support of the members of the REGARD Detector Physics Research Group of the Winger RCP.

References

[1] L.W. Alvarez et al., Science **167** 832, (1970).
[2] K. Borozdin, et al., Nature **422** 277, (2003).
[3] A. Orio-Alonso1, E. Alonso-González, C. Díez-González, P. Gómez-García1, P. Martínez-Ruiz, Geophysical Research Letters **50** 14, (2023)
[4] S. Vanini, P. Calvini, P. Checchia, A. R. Garola, J. Klinger, G. Zumerle, G. Bonomi, A. Donzella, A. Zenoni, Phil. Trans. R. Soc. **377** 20180051., (2019)
[5] H. Fujii et al., Progress of Theoretical and Experimental Physics Volume **2019** 5, (2019)
[6] D. Varga, G. Nyitrai, G. Hamar, L. Oláh, Advances in High Energy Physics, 1962317, (2016).
[7] L. Oláh, Sz. J. Balogh, Á. L. Gera, G. Hamar, G. Nyitrai, H. K. M. Tanaka, D.Varga, 14th Pisa meeting proceedings (2018)
[8] L. Oláh, H. K. M. Tanaka, G. Hamar, D. Varga, Journal of Disaster Research **14** 701, (2019)
[9] H K. M. Tanaka, L. Oláh, Phil. Trans. R. Soc. A.3772018014320180143, (2019)
[10] L. Oláh, H. K. M. Tanaka, Muography of magma intrusion beneath the active craters of Sakurajima volcano. Geophysical Monograph Series, **270**, 109–122., (2023)
[11] L. Oláh, G. G. Barnaföldi, G. Hamar, H. G. Melegh, G. Surányi, D. Varga, Advances in High Energy Physics, Vol. **560192**, (2013)
[12] L. Oláh, G. G. Barnaföldi, G. Hamar, H. G. Melegh, G. Surányi, D. Varga, Instrum. Method. Data Syst. **1** 229 (2012)
[13] H. K. M. Tanaka, K. Sumiya, L. Oláh., Geosci. Instrum. Method. Data Syst., **9**, 357–364, (2020)
[14] L. Oláh, G. Hamar, S. Miyamoto, H. K. M. Tanaka, D. Varga, BUTSURI TANSA, **71**, 161-168, (2018)
[15] L. Oláh, T. Mori, Y. Sakatani, H. K. M. Tanaka, D. Varga, iScience **26**, 108019, (2023)